JOURNAL OF BACTERIOLOGY, Mar. 1997, p. 1591–1597 Vol. 179, No. 5
0021-9193/97/$04.00+0

The Light Organ Symbiont *Vibrio fischeri* Possesses Two Distinct Secreted ADP-Ribosyltransferases

KARL A. REICH,† TERESA BIEGEL, AND GARY K. SCHOOLNIK*

Department of Microbiology and Immunology, Stanford University School of Medicine, Stanford, California 94305

Received 16 September 1996/Accepted 27 December 1996

We have previously described the purification, cloning, and initial characterization of a secreted ADP-ribosyltransferase, halovibrin (gene designation *hvn*), from the luminescent light organ symbiont *Vibrio fischeri*. This report describes a strategy for overexpression of halovibrin, the production and refinement of antihalovibrin antisera, and the molecular biological construction of a *V. fischeri* halovibrin null strain. Biochemical analysis of this mutant revealed that *V. fischeri hvn*^{null} still possessed ADP-ribosyltransferase activity and that this activity is immunologically, genetically, and structurally distinct from the previously described enzyme. This unusual finding, of two ADP-ribosyltransferase enzymes produced by a microorganism, is complemented by the details of the purification to apparent homogeneity and in vitro regulation of this new protein, halovibrin-β.

The luminescent marine bacterium *Vibrio fischeri* occupies several ecological niches that include the intestinal tracts of fishes, free living in the open ocean, and, for some strains, the light organ of various fish, and of squid species of the genus *Euprymna* (12, 19). This latter bacterium-host interaction has been adapted to the laboratory, where the specificity and interplay of symbiont-host interactions can begin to be addressed (15, 16, 18, 19).

The light organ *Vibrio-Euprymna* model has a number of structural, functional, and conceptual parallels with the mammalian intestine. These similarities include (i) an epithelium organized into villi and microvilli lining a topologically external cavity, (ii) a mucus layer that coats the host epithelial cells and envelopes the bacteria within the lumen of the light organ, and (iii) a regular, diurnal, contractile expulsion of excess microorganisms (19). The developmental parallel between the mammalian intestine and the light organ is particularly instructive, as the development of the light organ in hatchling squid is dependent on bacterial colonization by the correct species and strain of *V. fischeri* (13, 15), and in much the same fashion, the grossly underdeveloped digestive system of gnotobiotic mice assumes its regular appearance after its normal microbial flora are introduced (4). These are clear indications that in both systems bacterium-host communication is an essential part of the normal developmental process.

Previously, we have described the discovery, purification, cloning, and initial characterization of a secreted ADP-ribosyltransferase, halovibrin, produced by *V. fischeri* (17). In preparing reagents to study the potential role(s) of this signaling enzyme in the biology of symbiosis, we observed that *V. fischeri* secretes a second, apparently unrelated ADP-ribosyltransferase.

Our approach to exploring the function of halovibrin in the *V. fischeri-Euprymna scolopes* interaction included the expression of recombinant halovibrin, the production and refinement of polyclonal antisera directed against this protein, and the construction of *V. fischeri hvn*^{null} strains. Most interestingly, these mutant strains still possessed ADP-ribosyltransferase activity that could be readily assayed in the supernatant of stationary-phase cultures. This new secreted ADP-ribosyltransferase is immunologically, genetically, and structurally distinct from our first enzyme (now renamed halovibrin-α). In this report, we describe the experiments leading to the observation and purification of this new enzyme, halovibrin-β.

MATERIALS AND METHODS

ADP-ribosyltransferase assays. ADP-ribosyltransferase activity (14, 17) was assayed by using 1 mg of poly-L-arginine (Sigma) per ml in 25 mM sodium phosphate (pH 7.0)–20 mM dithiothreitol–10 μCi of [^{32}P]NAD (1,000 mCi/mmol; Amersham) per ml. Reaction mixtures (100 μl) were incubated for 3 h at 30°C. At this time, 50-μl aliquots were spotted onto individually numbered trichloroacetic acid-treated 3MM (Whatman) paper squares. These were washed twice with 5% trichloroacetic acid, dried in methanol, and counted in fluor (Ready-Safe; Beckman). Reactions were run in duplicate, using authentic cholera toxin (Sigma) as a standard.

Production of recombinant halovibrin-α. Overnight cultures of *Escherichia coli* DH5αF′/pET21b/Δ[1-26]*hvn*-α-6xHis were washed in phosphate-buffered saline (PBS) and diluted (1/25) into fresh medium containing 1 mM isothiogalactopyranoside (IPTG). After 4 h, cells from induced cultures were concentrated 50-fold by centrifugation and resuspension in 10 mM Tris-Cl–1 mM EDTA (pH 8.0). The bacteria were lysed by sonication (six times for 15 s each; Branson), and the cell lysate was centrifuged (16,000 rpm for 20 min) to recover the insoluble pellet.

Purification of recombinant halovibrin-α. The insoluble protein recovered from the cell lysate was solubilized in 6 M guanidinium-HCl in 0.1 M sodium phosphate (pH 8.0) and chromatographed at room temperature on an Ni-nitrilotriacetic acid affinity resin (Qiagen) equilibrated in the same buffer. The column was extensively washed in start buffer, and His-tagged Δ[1-26]halovibrin-α was specifically eluted in 6 M guanidinium-HCl with a three-step sodium phosphate pH gradient: pH 6.3, pH 5.9 and finally pH 4.5. The purification was monitored by sodium dodecyl sulfate (SDS)-polyacrylamide gel electrophoresis (PAGE) and Coomassie brilliant blue staining.

Renaturation of recombinant halovibrin-α. The most highly purified fractions obtained from the Ni-nitrilotriacetic acid affinity resin were diluted 1:5 in PBS and subsequently dialyzed against PBS (this last step performed at 4°C). Recombinant halovibrin-α was stable and active in our ADP-ribosyltransferase assay. This enzymically active material was purified further by ultrafiltration (Centriprep 10; Amicon) and preparative SDS-PAGE. Halovibrin-α was visualized by KCl staining and recovered by electroelution (2). After dialysis to remove excess SDS, the final gel-purified material was used as an antigen for the production of polyclonal antisera in rabbits (Josman Laboratories).

* Corresponding author. Mailing address: Stanford University Hospital, Department of Microbiology and Immunology, Beckman Center, Rm. B241, Stanford, CA 94304-5428. Phone: (415) 723-8158. Fax: (415) 723-1399.

† Present address: Abbott Laboratories, Abbott Park, IL 60064-3500.

TABLE 1. Bacterial strains and plasmids used

Strain or plasmid	Relevant characteristics	Reference or source
Bacterial strains		
V. fischeri ES114	Symbiotically competent light organ symbiont	3
V. fischeri ESR1	Rifampin-resistant variant of ES114	6
V. fischeri hvn-α^{null}	Halovibrin-α deletion strain of ESR1	This study
E. coli S17.1/λpir	RP4 *tra* functions	20
E. coli DH5αF′	Cloning host	New England Biolabs
Plasmids		
pACYC184	Tc^r Cm^r low-copy-number cloning vector	New England Biolabs
pET21b	His-tagged protein fusion vector	NovaGen
pUC19	Amp^r, cloning vector	Pharmacia
pBSKSII$^+$	Amp^r, cloning vector	Stratagene
pKNG101	Str^r Suc^s ori R6K suicide vector	8
pUC19/*Eco*RI	*V. fischeri Eco*RI fragment containing *hvn*-α cloned into pUC19	17
pUC19/*Pst*I	Downstream *Pst*I fragment cloned into pUC19	This study
pBSKSII$^+$/L	5′ *hvn*-α homologous region cloned into pBluescript	This study
pBSKSII$^+$/L+R	5′ and 3′ *hvn*-α homologous regions cloned into pBluescript	This study
pBSKSII$^+$/L+R/*cat*	Cm^r cassette cloned between 5′ and 3′ *hvn*-α homologous regions	This study
pKNG101/L+R/*cat*	Complete construction cloned into suicide vector	This study
pET21b/Δ*hvn*-α–6XHis	*hvn*-α lacking leader sequence, cloned into pET21b	This study
Recombinant *E. coli* strains		
S17.1/λpir/pKNG101/L+R/*cat*	*hvn*^{null} construction strain	This study
DH5αF′/pET21b/Δ*hvn*-α–6XHis	Δ[1–26]halovibrin-α expression strain	This study

Affinity purification of anti-halovibrin-α antibodies. Purified recombinant Δ[1-26]halovibrin-α-6xHis (see above) was dialyzed against PBS and coupled to cyanogen bromide-activated Sepharose 4B (Pharmacia) according to the manufacturer's instructions. Rabbit immunoglobulin was purified by repeated precipitation with ammonium sulfate (7) and, after dialysis against PBS, loaded onto the prepared halovibrin-α affinity column. The column was washed with 5 volumes of 1.0 M NaCl in PBS, and halovibrin-α-specific antibodies were eluted with a step gradient of acidic buffer (0.100 M glycine-HCl [pH 2.5]) followed by a step gradient of a basic buffer (0.100 M triethylamine-HCl [pH 11]). Fractions were neutralized immediately with an aliquot of 1.0 M Tris-Cl (pH 8.0) previously added to each tube. Fractions were analyzed by enzyme-linked immunosorbent assay (ELISA) (7), using bound halovibrin-α, and developed by using horseradish peroxidase-coupled goat anti-rabbit antisera (Amersham). ELISA-reactive fractions were pooled, dialyzed against PBS, concentrated by ultrafiltration (Centricon 30; Amicon), aliquoted, and frozen at −80°C.

Molecular biological techniques. DNA sequences were analyzed by using DNA Strider, GCG, and IG Suite. Standard conditions (1) were used for restriction enzyme digests, plasmid isolation, ligation reactions, subcloning, kinase treatment, transformations, random prime labeling, genomic DNA isolation, PCR, and Southern hybridizations.

Oligonucleotides used in this study. Oligonucleotides used to generate various fragments were as follows: Left homologous fragment, 5′-ATT AAT GTC GAC TAC TTC TTC CGA CAT TAT-3′ and 5′-ATT AAT TCT AGA GTA GAA CAA ACC AAC TGA-3′; Right homologous fragment, 5′-ATT AAT TCT AGA TAT TCA AAC CAA GAT GTA-3′ and 5′-ATT AAT GAG CTC GTC GAC TTT GCT ATG TCC CCA CTA-3′; *Xba*I chloramphenicol acetyltransferase gene (*cat*), 5′-ATT AAT CTG CAG ACC GGG TCG AAT GCT TTC-3′ and 5′-ATT AAT CTG CAG TAC CTG TGA CGG AAG ATC AC-3′; *hvn*-α, 5′-AAT AAT GAA TTC GAT GGA ATA TAT TAT GAA ATT TA-3′ and 5′-ATT AAT AAG CTT AAT TGC TTG TTC ATT CAT ATT-3′; Δ *hvn*-αhis: 5′-ATT AAT GAA TTC GGA TGA TGC TGC AGT AAG-3′ and 5′-ATT AAT AAG CTT AAT TGC TTG TTC ATT CAT ATT-3′; and internal *hvn*-α fragment, 5′-CAA ATG ATG ATG CTG CAG-3′ and 5′-ATA TAC ATA GAA GAA TGC-3′.

Cloning of downstream *Pst*I fragment. The genomic *Pst*I fragment adjacent to *hvn*-α on the *V. fischeri* chromosome was isolated by using the technique originally used to clone pUC19/*Eco*RI (17). Briefly, a size-selected library of *Pst*I-digested *V. fischeri* ES114 genomic DNA was constructed in a multicopy vector, and 1,000 recombinant clones were screened by Southern analysis in 20 pools of 50 clones with a gel-purified 1.2-kb *Pst*I fragment from pUC19/*Eco*RI (Table 1). Two cross-hybridizing clones were identified by this technique and subsequently isolated by repeated Southern analysis on progressively smaller pools of recombinant clones. Although cloned in both possible orientations, the DNA inserts appeared identical by restriction enzyme analysis, and one clone was chosen for DNA sequence analysis.

DNA sequencing. Dideoxy DNA sequencing was performed on double-stranded templates by using Sequenase (U.S. Biochemical) and universal primers and oligonucleotides derived from the sequence.

Western analysis. Samples were separated by SDS-PAGE (12% gel) and electrophoretically transferred (Genie Western; Idea Scientific) to Immobilon P (Millipore). Membranes were probed in 5% nonfat dry milk in 0.1 M Tris-Cl (pH 8.0) with affinity-purified anti-halovibrin-α antibodies (diluted 1/10,000), washed in 2.0 M NaCl in 0.1 M Tris-Cl (pH 8.0), and developed with horseradish peroxidase-coupled goat anti-rabbit antibodies (Amersham) and luminol (Dupont). Exposure times varied from 5 to 10 min.

Construction of pKNG101/L+R/*cat*. PCR primers were used to synthesize a 1,715-bp fragment containing a 5′ *Sal*I site and 3′ *Xba*I site. This DNA fragment consisted of 32 bp of *hvn*-α sequence and 1,683 bp of upstream sequence. PCR primers were also used to synthesize a second DNA fragment containing a 5′ *Xba*I site and 3′ adjacent *Sal*I and *Sac*I restriction sites. This 1,602-bp DNA fragment consisted of 53 bp of the 3′ end of *hvn*-α and 1,549 bp of downstream sequence. Using PCR primers that contained terminal *Xba*I restriction sites, the *cat* gene from pACYC184 (Table 1) was also generated. These DNA fragments were then assembled in sequential order: (i) the first fragment (the Left homologous arm) was cloned into *Sal*I- and *Xba*I-digested pBluescript SKII$^+$ (pBSKSII$^+$ [Table 1]), yielding pBSKSII$^+$/L (Table 1); (ii) the second fragment (the Right homologous arm) was cloned into *Xba*I/*Sac*I-digested pBSKSII$^+$/L, making clone pBSKSII$^+$/L+R (Table 1); and (iii) the *cat* gene was cloned into *Xba*I-digested pBSKSII$^+$/L+R, yielding clone pBSKSII$^+$/L+R/*cat*. Finally, the assembled fragments (L+R/*cat*) were isolated from pBSKSII$^+$/L+R/*cat* by *Sal*I digestion, gel purified, and cloned into *Sal*I-digested pKNG101 (Table 1), making pKNG101/L+R/*cat* (Table 1). This plasmid was then transformed into *E. coli* S17.1/λpir (Table 1).

Conjugations. Conjugations were performed by mixing equal volumes (150 μl) of washed overnight cultures of *E. coli* S17.1/λpir (Table 1) harboring pKNG101/L+R/*cat* and *V. fischeri* ESR1 (Table 1). The cells were pelleted, resuspended in 15 μl, incubated on LBS (17) agar plates for 2 h, resuspended in 600 μl of LBS, vortexed thoroughly, and spread on six LBS plates containing 100 μg of rifampin per ml, 3 μg of chloramphenicol per ml, and 5% sucrose. Exconjugants were reisolated on selective media and tested for streptomycin resistance. Streptomycin-sensitive strains were processed for genomic Southern analysis.

Purification of halovibrin-β. Overnight cultures of *V. fischeri hvn*-α^{null} were diluted 1/40 into 500 ml of fresh LBS in a 2-liter flask and grown for 15 h at 28°C at 200 rpm. Culture supernatant from 12 flasks was harvested by centrifugation (8,000 rpm for 30 min) and brought to 55% ammonium sulfate saturation (32.6 g/100 ml; UltraPure; ICN). The protein pellet was collected and resuspended in 100 ml of PBS. This solution was clarified by ultracentrifugation (2 h at 25,000 rpm in an SW28 rotor (Beckman), brought to a final concentration of 1.5 M ammonium sulfate, and loaded onto a 200-ml methyl-Sepharose (Pharmacia) hydrophobic interaction column prepared in 1.5 M $(NH_4)_2SO_4$ in 50 mM Tris-Cl (pH 8.0) buffer. This column was washed with start buffer and developed with a 1-liter reverse salt gradient from 1.5 to 0 M $(NH_4)_2SO_4$. The ADP-ribosyltransferase activity eluted early in the gradient and active fractions were pooled, dialyzed, and concentrated by ultrafiltration. This material was chromatographed on NAD-agarose (Sigma), and the ADP-ribosyltransferase activity was eluted with a step gradient of 1.5 M salt. This material was pooled and concentrated,

and buffer was exchanged in preparation for High S (Bio-Rad) fast protein liquid chromatography (FPLC). The column was prepared in 0.05 M sodium citrate (pH 5.1) buffer and developed with a linear 0 to 0.5 M NaCl gradient. ADP-ribosyltransferase activity eluted consistently at 0.110 M NaCl.

Media, growth conditions, and antibiotics. *V. fischeri* ESR1 was grown in LBS (17) with 100 μg of rifampin per ml at 28°C. *E. coli* strains were grown in LB (1) at 37°C with the appropriate antibiotic (ampicillin [100 μg/ml] or chloramphenicol [25 μg/ml]). All bacteria were grown with shaking (200 rpm).

Recovery of halovibrin-β activity after SDS-PAGE. A denaturing polyacrylamide gel with PDA (Bio-Rad) as the cross-linker was prepared a day in advance (2). Samples were mixed with Laemmli (10) sample buffer (prepared without reducing agent), loaded directly on the gel, and electrophoresed overnight at 50 V. The gel was soaked in 2% Triton X-100 in 25 mM Tris-Cl (pH 8.0) for 30 min with two changes of buffer. Strips, corresponding to individual lanes, were cut from the gel; sequential 0.5-cm slices were cut, diced, and incubated overnight in 100 μl of 1% Triton X-100 (Sigma) in 25 mM Tris-Cl (pH 8.0); and 10-μl aliquots were assayed for ADP-ribosyltransferase activity.

Silver staining. SDS-polyacrylamide gels were fixed in isopropanol-acetic acid-water (30:10:60) and prepared for alkaline-initiating silver staining as described previously (5).

RESULTS

Strategy for overexpression of recombinant halovibrin-α. To obtain biologically active halovibrin-α for structure-function analysis, we chose to express this ADP-ribosyltransferase in an *E. coli* expression system capable of producing large amounts of protein (pTrc99A and pGEX [Pharmacia], pQE30 [Qiagen], and pMal-c2 and pMal-p2 [New England Biolabs]). Using specific PCR primers, we amplified the complete amino acid coding region of *hvn*-α and attempted to clone this DNA fragment into the above-mentioned vectors; transformants were exceedingly rare and, when obtained, were unstable and/or contained large rearrangements of vector and insert sequences (data not shown). This was surprising, since our original ADP-ribosyltransferase clone, pUC19/*Eco*RI, was stable and conferred ADP-ribosyltransferase activity to *E. coli* (17). We hypothesized that our failure to clone full length *hvn*-α in a high protein expression vector could be due to either (i) its intrinsic ADP-ribosyltransferase activity or (ii) deleterious interactions between its unconventional amino acid leader sequence and the secretory apparatus of *E. coli*. We tested these hypotheses by designing two new PCR primers that would permit the directed cloning of either full-length halovibrin-α or a truncated version of Hvn-α lacking the first 26 amino acids (Δ[1-26]halovibrin-α, gene designation Δ[1-26] *hvn*-α) into the well-regulated pET T7 expression system (Table 1). The results of this experiment (data not shown) indicated that only Δ[1-26]halovibrin-α could be cloned into this expression system, supporting the notion the halovibrin-α leader sequence might be toxic in some way to *E. coli*. Clones of pET21b/Δ[1-26]hvn-α-6xHis (Table 1) were stable and upon induction synthesized large amounts of recombinant protein that could be purified and renatured to full enzymatic activity (see Materials and Methods). Therefore, the protein obtained from clones of *E. coli* DH5αF′/pET21b/Δ[1-26]hvn-α-6xHis was used for all subsequent biochemical characterization, including antibody production and refinement (see Materials and Methods).

Construction of *V. fischeri* halovibrin-α null strain. To construct a specific *hvn*-α mutant in a symbiotically competent *V. fischeri* strain, we chose a gene replacement strategy that was designed to delete the coding region of *hvn*-α and substitute it with an antibiotic resistance gene. Because *V. fischeri* ES114 is naturally resistant to ampicillin (up to 1,000 μg/ml), kanamycin (150 μg/ml), and streptomycin (200 μg/ml) and fails to develop resistance to tetracycline, we chose to use the chloramphenicol acetyltransferase gene (*cat*) as the replacement gene. This targeted approach left both the upstream and downstream flanking genomic sequences of *hvn*-α intact, thus yielding a defined mutant strain that could be analyzed biochemically and tested for symbiotic competence.

We made use of a suicide vector (pKGN101 [Table 1]) containing selectable markers for the in vivo selection of clones in which a double recombination event would have produced an *hvn*-α gene replacement (Fig. 1). Prior experience in constructing directed mutants of symbiotically competent *V. fischeri* ES114 (unpublished results) led us to estimate that the inferred recombinations in Fig. 1 would require flanking homologous DNA fragments at least 1.4 kb in length. Sufficient sequence data for the design and construction of an upstream flanking region were available from our analysis of pUC19/*Eco*RI (Table 1), but as *hvn*-α is at the 3′ end of this DNA fragment (17), we lacked sufficient sequence information for the design and construction of a downstream flanking homologous fragment. Southern analysis of *V. fischeri* genomic DNA, probed with a 3′-terminal fragment from pUC19/*Eco*RI, showed that the adjacent genomic *Pst*I fragment would be large enough to provide a sufficiently long 3′ flanking fragment (data not shown). Using conventional techniques, this genomic *Pst*I fragment was cloned and sequenced (see Materials and Methods).

With this information in hand, a recombinant clone consisting of 1,733 bp of sequence upstream of *hvn*-α (Left homologous arm) and 1,633 bp of downstream sequence (Right homologous arm) separated by the *cat* gene was constructed (see Fig. 1 and Materials and Methods). This tripartite DNA fragment was cloned into pKNG101, transformed into *E. coli* S17.1/λpir and transferred to *V. fischeri* ESR1 (Table 1) by conjugation (see Materials and Methods). Conjugation mixtures were plated onto selective media, and the resulting colonies were reisolated and analyzed by Southern blotting.

Genomic DNA isolated from wild-type *V. fischeri* ESR1 and from three independently isolated *V. fischeri* derivatives that were predicted to contain the *hvn*-α^{null} mutation were probed with ^{32}P-labeled Left and Right homologous arms (Fig. 2A). Restriction enzymes were chosen to detect possible disruption(s) of sequences upstream and downstream of *hvn*-α (*Eco*RI), loss of the *hvn*-α coding region (*Pst*I), and the introduction of the *cat* antibiotic resistance marker (*Xba*I). The results of this restriction fragment length analysis (Fig. 2A) show that the upstream and downstream regions of the three mutants were unaffected; the bands seen in the mutants after *Eco*RI digestion were the expected size and identical to that seen in wild type. The chromosomally introduced *cat* gene has one *Eco*RI site (Fig. 1), and thus after *Eco*RI digestion, a new 800-bp DNA fragment would be expected to cross-hybridize with the Right homologous arm. However, because this DNA fragment has only 300 bp of homologous sequence with the right flanking arm, it is not visible in Fig. 2. Longer autoradiographic exposures and the use of high-specific-activity DNA probes revealed the expected 800-bp fragment (data not shown). The replacement of the *hvn*-α coding region was diagnosed by the concomitant loss of an internal *Pst*I site; the wild-type pattern of two bands should be reduced to a single *Pst*I fragment whose size is the sum of the sizes of the two wild-type bands (2.11 + 5.4 kb); the restriction fragment pattern of the three mutants shows the expected change (Fig. 2A). The presence of the *cat* gene can be conveniently monitored by using the PCR-generated *Xba*I sites that flank this gene; the wild-type pattern of a single band upon *Xba*I digestion should be converted to two bands in the mutants, the sum of whose sizes should equal the size of wild-type band. The three independently isolated mutants show the expected restriction fragment length pattern (Fig. 2A). As an additional test for the loss of *hvn*-α sequences, the nylon membrane used to generate the autoradiogram in Fig. 2A was stripped and reprobed with a

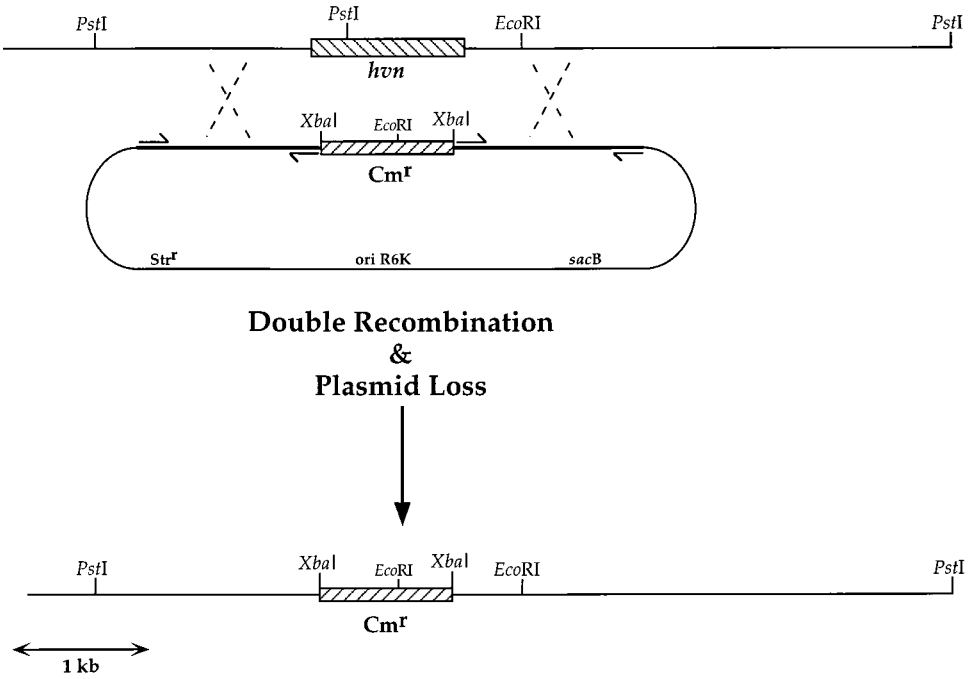

FIG. 1. Design and construction of *V. fischeri hvn*-α^{null} strain. (Top) The upper line shows a partial restriction map of the *hvn* region on the *V. fischeri* chromosome and the amino acid coding region of halovibrin-α (hatched box). (Middle) Suicide vector pKNG101/L+R/*cat* is shown with the Right and Left homologous arms (heavy line) and the position of the intervening *cat* gene. Plasmid sequences are not drawn to scale. Two possible homologous recombination events which would lead to *hvn* gene replacement are indicated by the dashed lines. (Bottom) Partial restriction map of the *V. fischeri hvn*-α^{null} strain. Note positions of *Eco*RI, *Pst*I, and *Xba*I restriction sites. See text for details.

gel-purified, PCR-generated, internal *hvn*-α DNA fragment; as expected, only wild-type genomic DNA produces a signal with this probe (Fig. 2B), whereas no hybridizing fragment is detected in genomic DNA from the three mutants, even after longer exposure times. We interpret these data as formal proof for the construction of a genetic null for *hvn*-α in *V. fischeri* and as evidence that the surrounding genetic milieu of *hvn*-α is unaltered in these strains.

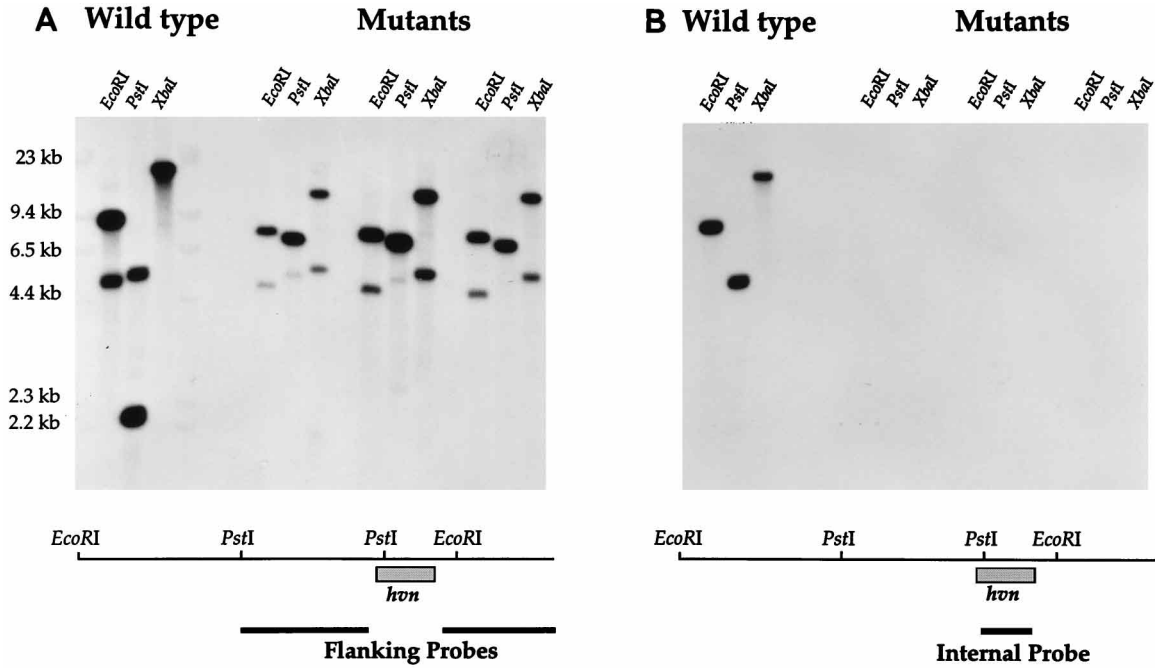

FIG. 2. Genomic Southern analysis of *V. fischeri* wild type and *hvn*-α^{null} strains. Shown is an autoradiogram of *V. fischeri* genomic DNA digested with the indicated enzymes, separated by agarose gel electrophoresis, and transferred to nylon membrane. (A) Membrane probed with radiolabeled Left and Right homologous arms; (B) autoradiogram of same membrane after stripping and reprobing with *hvn*-α internal DNA probe. A partial restriction map of the *hvn*-α region and the positions of the relevant DNA probes are indicated beneath each panel.

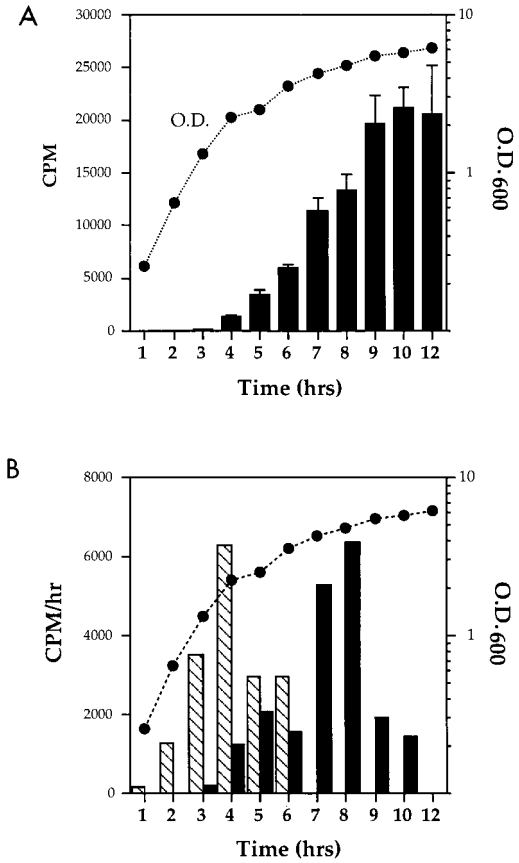

FIG. 3. ADP-ribosyltransferase activity from *V. fischeri hvn*-α^{null}. (A) The ADP-ribosyltransferase activity in the supernatant of 50-ml cultures of *V. fischeri hvn*^{null} was measured at the indicated times. The optical density at 600 nm (O.D.600) of the cultures is also shown (circles). Assays were done in triplicate, and error bars, when larger than symbols, are shown. (B) Rate of production of ADP-ribosyltransferases in wild-type *V. fischeri* as a function of bacterial growth. ADP-ribosyltransferase activities due to halovibrin-α (hatched bars) and halovibrin-β (solid bars) are shown. The optical densities at 600 nm of the matched wild-type and mutant cultures (circles) are shown.

Secretion of a second ADP-ribosyltransferase by the *V. fischeri hvn*-α^{null} mutants. Although the molecular biological evidence for our construction of a *hvn*-α null strain (see above) was compelling, we nonetheless sought additional evidence for the loss of *hvn*-α by testing the supernatant from *V. fischeri hvn*-α^{null} cultures for ADP-ribosyltransferase activity and for proteins recognized by an affinity-purified antiserum to halovibrin-α (see Materials and Methods). No cross-reacting proteins were detected by Western blotting (data not shown). However, to our surprise, significant ADP-ribosyltransferase activity was detected in *V. fischeri hvn*-α^{null} culture supernatants (Fig. 3A). This observation was confirmed by assaying each of the three independently derived null strains. High levels of ADP-ribosyltransferase activity could be assayed from the supernatant, and all three isolates gave identical results. Further, and in contrast to Hvn-α, this new activity was produced during the stationary phase of growth of in vitro-grown *V. fischeri* (Fig. 3A). This finding, and the antigenic difference from Hvn-α, establishes the activity as a second ADP-ribosyltransferase activity, which we have designated halovibrin-β.

Halovibrin-α and halovibrin-β are differentially expressed during the exponential and stationary growth phases of *V. fischeri*. The ADP-ribosyltransferase activity measured from cultures of *V. fischeri* will be the sum of the activities of Hvn-α and Hvn-β and any additional (i.e., non-α, non-β) ADP-ribosyltransferase that may be expressed. Using matched cultures of wild-type and *hvn*-α^{null} *V. fischeri* strains, and subtracting the contribution of Hvn-β from the total ADP-ribosyltransferase activity, we were able to deduce the contributions of Hvn-α and Hvn-β (plus any other ADP-ribosyltransferase) to the total measured activity. Expressed as the rate of production of ADP-ribosyltransferase activity per hour, this approach demonstrated that the two *V. fischeri* ADP-ribosyltransferases were differentially regulated: Hvn-α was secreted during the exponential phase of growth, whereas Hvn-β (plus any other non-α, non-β ADP-ribosyltransferase) was selectively produced during the stationary phase of growth (Fig. 3B). This conclusion, which assumes that (i) the growth phase-dependent expression of Hvn-β is the same in an *hvn*-α^{null} strain as in the wild-type parent strain and (ii) the specific activities of the two enzymes are roughly comparable, was confirmed by semiquantitative Western analysis of concentrated wild-type supernatant, using affinity purified anti-halovibrin-α antibodies (data not shown), and by the purification of Hvn-β (see below). This pattern of differential expression was seen in all three of the *hvn*-α^{null} strains.

Purification of halovibrin-β. To characterize halovibrin-β biochemically, we purified the ADP-ribosyltransferase activity produced by *V. fischeri hvn*-α^{null} (see Materials and Methods). Briefly, supernatant from stationary-phase cultures was collected and concentrated by ammonium sulfate precipitation. This material was resuspended, clarified by ultracentrifugation, and subjected to sequential hydrophobic, affinity, and anion-exchange chromatography. Final purification of halovibrin-β was accomplished by preparative SDS-PAGE. Superficially, this purification scheme resembles that used for halovibrin-α (17); however, the details of the methods differ considerably. These differences, which indicate that the two enzymes have different biochemical properties, include the use of different hydrophobic interaction resins (phenyl versus methyl), different NAD agarose affinity matrices (ligand attachment by ribose hydroxyls versus N-6 linkage), and different elution pHs from the High S cation exchange column (pH 5.50 versus pH 5.10). The protein profiles of the individual purification steps are shown in Fig. 4A.

Recovery of halovibrin-β ADP-ribosyltransferase activity after SDS-PAGE. Although the molecular weight of the final major protein band seen on SDS-PAGE and silver staining (Fig. 4) matched the estimated molecular weight of our activity as measured by gel permeation FPLC (data not shown), we sought additional evidence to identify the band possessing ADP-ribosyltransferase activity. Active fractions from High S FPLC were pooled, concentrated by ultrafiltration, and separated by nonreducing SDS-PAGE. After electrophoresis, excess SDS was removed (see Materials and Methods) and sample lanes were cut into sequential 0.5-cm strips, eluates from which were assayed for activity. The results (Fig. 5) show that halovibrin-β retained activity after nonreducing SDS-PAGE and that this activity coincides with the major 32-kDa protein. All of the measured ADP-ribosyltransferase activity was found in fractions 6 and 7, with a total recovery of 48%. The recovery of halovibrin-α ADP-ribosyltransferase activity after SDS-PAGE was always less than 0.5% under all conditions tested. An incidental observation was that halovibrin-β undergoes a molecular mass shift (~3 kDa smaller) when electrophoresed under reducing conditions compared to the molecular mass seen under nonreducing SDS-PAGE.

Halovibrin-β is immunologically distinct from halovibrin-α. To verify the immunological difference between the two halovi-

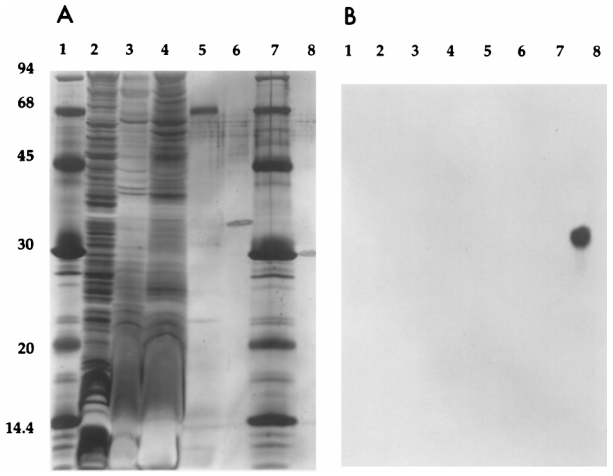

FIG. 4. SDS-PAGE and Western analysis of purified ADP-ribosyltransferases from *V. fischeri*. (A) Fractions obtained during the purification of Hvn-β were separated by SDS-PAGE and visualized by silver staining. Lanes: 1 and 7, molecular weight standards; 2, culture supernatant from *V. fischeri hvn*-α^{null}; 3, hydrophobic interaction chromatography pooled peak; 4, NAD-agarose pooled peak; 5, High S FPLC peak; 6, SDS-PAGE eluate; 8, Δ[1-26]halovibrin-α-6xHis. (B) Western analysis of the gel shown in panel A. An identical gel was transferred to Immobilon P and probed with affinity-purified anti-halovibrin-α antibody. Sizes are indicated in kilodaltons.

brins, various fractions from the halovibrin-β purification were separated by SDS-PAGE, transferred to a membrane, and probed with affinity-purified anti-halovibrin-α antibodies (see Materials and Methods). No cross-reacting bands were observed in any of these protein fractions, confirming that the two secreted ADP-ribosyltransferases have different apparent molecular weights (Fig. 4A) and are immunologically distinct (Fig. 4B). Electrophoretic transfer was monitored by using prestained molecular weight standards and confirmed by membrane staining with amido black.

DISCUSSION

From our observation of a secreted ADP-ribosyltransferase activity from the nonpathogenic light organ symbiont *V. fischeri* (17), we had anticipated finding, and had experimental evidence for, other ADP-ribosyltransferases in a number of other marine bacterial species. Although there is no a priori reason for an organism to be limited to a single ADP-ribosyltransferase, and there is at least one example of a multiplicity of these enzymes being made by a single bacterium (ExoA, ExoS, and ExoS-like proteins in *Pseudomonas aeruginosa* [9]), we were surprised that by analyzing *V. fischeri* we uncovered another member of this family of bacterial signaling enzymes.

Our experimental approach of recombinant overexpression of halovibrin-α, production of immunological reagents, and the construction of a targeted genetic null strain led directly to our observation of a second ADP-ribosyltransferase secreted by *V. fischeri*. This new enzyme is immunologically distinct from halovibrin-α although it catalyzes the same in vitro enzymatic reaction.

The conditions used to purify Hvn-β were different from those used to isolate Hvn-α; these differences include distinct affinity resins, ion-exchange elution conditions, and recovery of ADP-ribosyltransferase activity after SDS-PAGE. We interpret these distinguishing biochemical markers as evidence for structural differences in the surface charge and active sites of these two proteins. As secreted bacterial ADP-ribosyltransferases catalyze identical reactions (the transfer of the adenosine diphospho-ribose moiety of NAD to eucaryotic proteins), we speculate that these biochemical differences are evidence for different host targets modified by Hvn-α and Hvn-β.

Antibodies directed against recombinant Hvn-α were Western blot reactive against authentic Hvn-α purified from *V. fischeri* and recognized Hvn-α in culture supernatants and in biological samples prepared for immunoelectron microscopy (17a). These antibodies were not enzymatically neutralizing and did not react with Hvn-β. The lack of immunological cross-reactivity between Hvn-α and Hvn-β in conjunction with our failure to observe any cross-hybridizing bands with *V. fischeri* genomic DNA probed with *hvn*-α is interpreted as further evidence that Hvn-α and Hvn-β will prove to be, at most, only partially related.

We present data that show that Hvn-α and Hvn-β are produced at different phases of bacterial growth: halovibrin-α is secreted during exponential growth, and halovibrin-β appears in stationary phase. The differential regulation of these enzymes could be a clue to the potential role(s) that they play in the biology of symbiosis. Interestingly, the colonizing bacteria of the *Euprymna scolopes* light organ follow a diurnal cycle which includes the exponential growth of *V. fischeri* within the light organ, followed by an expulsion of stationary-phase organisms that have completely filled the light organ (11). We note that the functions that these two secreted ADP-ribosyltransferases play in the biology of symbiosis could be derived not only from their different possible eucaryotic protein targets but also from their differential regulation in *V. fischeri* (Fig.

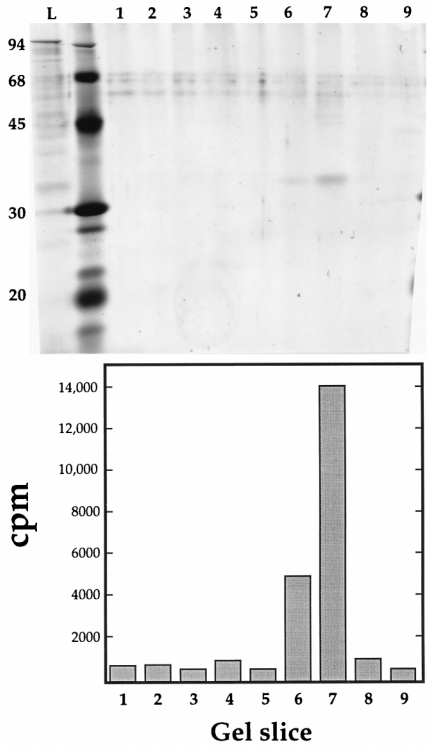

FIG. 5. Recovery of Hvn-β ADP-ribosyltransferase activity after SDS-PAGE: correlation of activity with 32-kDa protein. (Top) Silver-stained SDS-polyacrylamide gel. Lanes: L, High S FPLC pool sample lane; 1 to 9, eluate from sequential 0.5-cm slices of sample lane separated by SDS-PAGE; 2, molecular weight standards. (Bottom) ADP-ribosyltransferase activity assayed from the indicated gel slice.

3B). In this way, the bacterial symbiont could be the controlling partner in the symbiotic interaction.

We have recently screened a collection of bacterial symbionts collected from the light organs of a variety of fish and squid species for ADP-ribosyltransferase activity and Hvn-α- and Hvn-β-like genes and proteins. The results of this preliminary study show that these genes, proteins, and activities are present (in various combinations) in all of the symbionts that we have tested. This observation, along with our discovery of Hvn-β, enhances the likelihood that development of the *Euprymna scolopes* light organ is influenced by the interplay of Hvn-α and Hvn-β with host target tissues. It is possible that ADP-ribosyltransferases are communication signals for an entire class of marine bacterium-host interactions and that other, nonpathogenic bacteria will be found to have members of this family of enzymes as well.

ACKNOWLEDGMENTS

This work was supported in part by the Howard Hughes Medical Institute.

We thank Sandra Ramer, David Bieber, and Ned Ruby for critical reading of the manuscript and Michele Nishiguchi for providing strains in advance of publication.

REFERENCES

1. **Ausubel, F. M., R. Brent, R. E. Kingston, D. D. Moore, J. G. Seidman, J. A. Smith, and K. Struhl (ed.).** 1991. Current protocols in molecular biology. John Wiley & Sons, New York, N.Y.
2. **Bhown, A. S., and J. C. Bennett.** 1983. High sensitivity sequence analysis of proteins recovered from sodium dodecyl sulfate gels. Methods Enzymol. **91:**450–455.
3. **Boettcher, K. J., and E. G. Ruby.** 1990. Depressed light emission by symbiotic *Vibrio fischeri* of the sepiolid squid *Euprymna scolopes*. J. Bacteriol. **172:** 3701–3706.
4. **Coates, M. E.** 1975. Gnotobiotic animals in research: their uses and limitations. Lab. Anim. **9:**275–82.
5. **Giulian, G. G., R. L. Moss, and M. Greaser.** 1983. Improved methodology for analysis and quantitation of proteins on one-dimensional silver-stained slab gels. Anal. Biochem. **129:**277–287.
6. **Graf, J., P. V. Dunlap, and E. G. Ruby.** 1994. Effect of transposon-induced motility mutations on colonization of the host light organ by *Vibrio fischeri*. J. Bacteriol. **176:**6986–6991.
7. **Harlow, E., and D. Lane.** 1988. Antibodies, a laboratory manual. Cold Spring Harbor Laboratory, Cold Spring Harbor, N.Y.
8. **Kaniga, K., I. Delor, and G. R. Cornelis.** 1991. A wide host-range suicide vector for improving reverse genetics in Gram-negative bacteria: inactivation of the *blaA* gene of *Yersinai enterocolitica*. Gene **109:**137–141.
9. **Krueger, K. M., and J. T. Barbieri.** 1995. The family of bacterial ADP-ribosylating exotoxins. Clin. Microbiol. Rev. **8:**34–47.
10. **Laemmli, U. K.** 1970. Cleavage of structural proteins during the assembly of the head of bacteriophage T4. Nature **227:**680–685.
11. **Lee, K. H.** 1995. Symbiotic role of the viable but nonculturable state of *Vibrio fischeri* in Hawaiian coastal seawater. Appl. Environ. Microbiol. **61:**278–283.
12. **Lee, K. H., and E. G. Ruby.** 1992. The detection of squid light organ symbiont *Vibrio fischeri* in Hawaiian seawater by using *lux* gene probes. Appl. Environ. Microbiol. **58:**942–947.
13. **McFall-Ngai, M. J., and E. G. Ruby.** 1991. Symbiont recognition and subsequent morphogenesis as early events in an animal-bacterial mutualism. Science **254:**1491–1494.
14. **Mekalanos, J. J.** 1988. Production and purification of cholera toxin. Methods Enzymol. **165:**169–175.
15. **Montgomery, M. K., and M. McFall-Ngai.** 1994. Bacterial symbionts induce host organ morphogenesis during early postembryonic development of the squid *Euprymna scolopes*. Development **120:**1719–1729.
16. **Montgomery, M. K., and M. McFall-Ngai.** 1993. Embryonic development of the light organ of the sepiolid squid *Euprymna scolopes* Berry. Biol. Bull. **184:**296–308.
17. **Reich, K. A., and G. K. Schoolnik.** 1996. Halovibrin, secreted from the light organ symbiont *Vibrio fischeri*, is a member of a new class of ADP-ribosyltransferases. J. Bacteriol. **178:**209–215.

17a. **Reich, K. A., A. Small, and M. McFall-Ngai.** Unpublished observation.

18. **Ruby, E. G., and L. M. Asato.** 1993. Growth and flagellation of *Vibrio fischeri* during initiation of the sepiolid squid light organ symbiosis. Arch. Microbiol. **159:**160–167.
19. **Ruby, E. G., and M. J. McFall-Ngai.** 1992. A squid that glows in the night: development of an animal-bacterial mutualism. J. Bacteriol. **174:**4865–4870.
20. **Simon, R., M. O'Connell, M. Labes, and A. Pühler.** 1986. Plasmid vectors for the genetic analysis of and manipulation of *Rhizobia* and other Gram-negative bacteria. Methods Enzymol. **118:**640–659.